DNS/LES FOR COMPLEX FLOWS AND INDUSTRIAL INTEREST

P. SAGAUT
ONERA
29 av. de la division Leclerc, 92322 Châtillon cedex, France
Tel : 33 (0)1 46 73 42 71
email : sagaut@onera.fr

Abstract.

This paper presents a general overview of the recent works dealing with LES/DNS carried out at ONERA. The emphasis is put on developments aiming at extending or using these techniques for complex flows directly connected with practical applications.

1. Introduction

Unsteady numerical simulation of flows of theoretical and practical interest is more and more popular. It allows us to gain a deeper insight in involved physical mechanisms, and practical experience shows that it reduces the constraint on the turbulence modeling (when compared to steady RANS computations), since a significant part of the turbulent motion is directly captured. Main drawbacks are that the solution is often much more sensitive to numerical errors than steady RANS computations and that huge amounts of grid points is needed to obtain a satisfactory solution.

The rapid increase of the computing power makes it now possible to perform DNS and/or LES of complex flows, which cannot be considered as "academic test cases".

In this paper, we will discuss some applications of DNS and/or LES to flows of practical interest performed at ONERA :

- Subsonic flow around a two-dimensional wing near stall.
- Flow around a Delta wing with vortex breakdown.
- Flow around a low-pressure turbine blade.

For all these applications, the parameters of the wind-tunnel experiments (geometry, Reynolds number) are strictly reproduced in the simulations. All these flows involve a wide range of physical phenomena, such as transition, separation, boundary layer, wake, etc. As a consequence, they are challenging cases for LES and DNS, since they cannot be treated with one of these approaches only. Because of the high value of the Reynolds number (up to several millions in some cases), a full DNS cannot be employed over the whole computational domain, and LES must be used. But transitional region must be treated with DNS or quasi-DNS resolution. This kind of complex applications thus requires the development of hybrid approaches, based on self-adaptive subgrid models and *ad hoc* numerical techniques, which must be able to provide some numerical stabilization without polluting the solution.

New developments dealing with zonal multiresolution DNS/LES techniques are presented in Sec. 2. Problems dealing with the control of numerical dissipation are discussed in Sec. 3. Results dealing with the previously mentioned applications and obtained making use of the zonal techniques are presented in Sec. 4. Then, new ways to reduce the computational cost of DNS/LES are discussed in Sec. 5.

2. Development of zonal multiresolution DNS/LES techniques

Most of the known works dealing with LES (see [1] for a recent review) and DNS on structured meshes make use of monodomain numerical algorithm, or conformal multidomain approach. This results in a severe limitation in the capability to concentrate the computational nodes in areas where important physical mechanisms occur while keeping the total number of grid points as low as possible. This limitation renders the use of classical DNS/LES approaches very expensive for complex geometries, where these "important areas" are very small when compared to the full geometry. This is well known for the classical example of the turbulent boundary layer.

In order to alleviate this problem, a zonal multiresolution approach has been developped [18], which in practice appears as a non-conformal subdomain technique. From the theoretical point of view, this approach leads to the problem of the coupling of two solutions with different filter lengths at the subdomain interface. It can be shown that, in the most general case, neither the instantaneous field nor the mean or rms fields are continuous at the interface, because of the difference in the filters. As a consequence, classical conservative treatments of the interface are no longer valid.

The proposed method rely on the definition of two operators at the interface: a restriction operator (from fine to coarse subdomains), and an

enrichment operator (from coarse to fine subdomains) to reconstruct the high frequencies on the interface. The restriction operator is defined as a filter applied to the high frequency solution. The enrichment algorithm is based on the extrapolation of the difference between the solution in the two subdomain near the interface. This algorithm was demonstrated to be efficient for filter length ratio as high as 4 for wall bounded turbulent flows (plane channel, 2D wings or delta wing).

The use of this technique has been extended to the definition of coupling between 2D and 3D subdomains [15]. This extension makes it possible to reduce the number of grid points for flows around 2D profiles by using 3D subdomains in turbulent zones only (boundary layer, wake), while 2D domains are defined everywhere else.

3. About the control of numerical dissipation

Another important problem which occurs for high Reynolds number complex flows is the stabilization of the simulation. Daily experience shows that subgrid models (even the most dissipative ones) do not prevent the occurance of spurious wiggles. This is even more obvious when transonic flows are aimed [7, 8, 9].

For schock-free flows, a modified version of the AUSM+(P) scheme has been developped [15]. This modification is based on the introduction of a wiggle detector, the dissipative part of the AUSM scheme being set to zero at locations where no wiggles are detected. This wiggle detector Φ is computed as follows in cell number i :

$$\Delta_{\phi}^{i} = \begin{cases} -1 & \text{if} \quad (\phi_{i+2} - \phi_{i+1})(\phi_{i+1} - \phi_{i}) < 0 \\ 1 & \text{otherwise} \end{cases} \tag{1}$$

$$W_{\psi_k} = \begin{cases} 1 & \text{if} \quad \Delta_{\psi_k}^{i} + \Delta_{\psi_k}^{i+1} < 0 \quad \text{or} \quad \Delta_{\psi_k}^{i} + \Delta_{\psi_k}^{i-1} < 0 \\ 0 & \text{otherwise} \end{cases} \tag{2}$$

The sensor is then defined as $\Phi = Max(W_{\psi_k}), k = 1, .., 5$, where ψ is the primitive variable vector. This sensor was shown to yield a very large reduction of the amount of numerical dissipation, preventing a possible conflict with the true subgrid dissipation induced by the models, as observed for classical upwind schemes [6, 17]. When MILES [2, 5] computations are wanted, the sensor is set to 1 everywhere.

When shocks are present, it is necessary to use some numerical stabilization. High-order ENO filters have been developped [8], which lead to an important cost reduction (up to a factor 15) when compared to classical ENO schemes. These filters are localized near discontinuities thanks to the use of a shock detector based on the proposal of Ducros *et al.* [4].

4. Examples of application

We now present three applications, which are good examples of recent achievements of LES/DNS at ONERA. All these simulations have been carried out using the multidomain/multiresolution technique and the wiggle detector describe above.

4.1. FLOW AROUND A TWO-DIMENSIONAL WING NEAR STALL

The first computational case is related to the flow around the Aerospatiale A-airfoil near stall (the angle of attack is equal to 13.3°). The chord Reynolds number is equal to 2.1 10^6. This case was selected during the LESFOIL project, and details of ONERA's results can be found in Ref. [15]. This configuration represents a challenging test case for both RANS and LES computations because of the complexity of the suction side boundary layer: the adverse pressure gradient induces a laminar separation with turbulent reattachment near the leading edge, and a massive separation occurs at the trailing edge.

The best results have been obtained when the transition process was directly captured by the simulation, i.e. when the grid in the boundary layer region was fine enough to represent the small scale physics. The corresponding grid contains 2048 points on the suction side, yielding $\Delta x^+ \approx 100$ everywhere. In the two other direction, the following criteria were fulfilled: $\Delta y^+ \leq 20$ and $\Delta z^+ \leq 2$. The total number of grid points is 7.2 millions. The corresponding number of grid points required to get the same grid resolution with a monodomain C mesh is 21 millions.

Good results have been obtained using the Mixed Scale Model [20, 11, 12, 1]. Pressure and friction coefficients are compared with experimental data in Fig. 1. Computed lift and drag are 1.539 and 0.0250, respectively. These values compare favourably with experimental results: 1.548-1.515 and 0.0206-0.0308, respectively.

With the same resolution, MILES results are less accurate but still reliable, mainly because the transition is affected. This is in agreement with the results of Mossi and Sagaut [17] for the plane channel case.

4.2. FLOW AROUND A DELTA WING WITH VORTEX BREAKDOWN

The flow around a Delta wing at high angle of attack with vortex breakdown is an example of 3D geometry. The Reynolds number based on the chord and the angle of attack are equal to 1.5 10^6 and 27^0, respectively. We present here the results obtained using the MILES approach, which is a good candidate for this kind of application involving massive separation and nearly-free shear layer dynamics.

The total number of subdomains is equal to 21, corresponding to 4 millions grid points. The equivalent number of grid points with a conformal subdomain technique is 200 millions. In order to reduce the number of grid points, a coarse grid was used in the near-wall region and a wall-model was employed to provide boundary conditions on solid walls.

A general view of the instantaneous flow is shown in Fig. 2, where the vortex breakdown is clearly observed. Mean velocity profile is compared with experimental data in Figs. 3 and 4, showing a satisfactory agreement.

4.3. FLOW AROUND THE T106 LOW-PRESSURE TURBINE BLADE

The last example deals with the transitional flow around the T106 low-pressure turbine blade, at a chord Reynolds number equal to 1.6 10^5. The inlet flow angle and the exit flow angle are equal to 37.7 and -63.2 degrees, respectively. The pitch to chord ratio is taken equal to 0.799. The computational setup corresponds exactly to the experimental configuration. This example is characterictic of applications which can be treated using both DNS and LES. Extensive DNS simulations have been performed by Durbin and his coworkers [3] on the same geometry, and the idea was here to reduce the number of grid points while preserving the quality of the results.

Once again, the grid was fine enough to capture durectly the transition process: $\Delta x^+ < 40$, $\Delta y^+ < 20$ and $\Delta z^+ < 1$, corresponding to the use of 920 grid points on the profile. The total number of grid points is reduced to 1 million, thanks to the use of 2D subdomain and progressive mesh refinement in the 3D zone along the profile based on the zonal multiresolution technique. The total number of subdomains is five 2D domains and six 3D domains. This is to be compared to the 25.10^6 points grid used for DNS at CITS.

A general view of the instantaneous flow is presented in Fig. 5. The transition process and the topology of the wake are clearly identified. Results of both MILES and classical LES (using the Mixed Scake Model) are compared with experimental results in Fig. 6. It is observed that a general very good agreement is recovered. An interesting point is that the two approaches yield the same results. This can be explained by the fact that the grid resolution is very good (meshes are at most twice larger as in the DNS grid), leading to very small subgrid effects. The discrepancy with the conclusion drawn from the A-profile simulations could be explained by the fact that the size of the mesh in streamwise direction is twice smaller in the blade case than in the wing computation, and the Reynolds number in smaller.

5. Further reduction of the computational cost

The applications presented above make use of the zonal multiresolution technique, but they all rely on the usual LES/DNS approaches. Further reduction of the CPU cost can be obtained thanks to the coupling of DNS/LES with new methods. We discuss here some approaches dealing with the coupling of LES with multilevel algorithms and two ways of performing RANS/LES coupling, which have not yet been applied to complex configurations.

5.1. MULTILEVEL ALGORITHMS

A possible way to reduce CPU cost of the LES approach is to define a multilevel algorithm [13], than can be interpreted as a time-consistant extension of the usual multigrid algorithm. The resulting method can be considered both as an acceleration technique and a new way to close the filtered Navier-Stokes equations without making use of the subgrid viscosity approach. In practice, N levels of embedded grids are defined, each one corresponding to a different filtering level. The key points of the method are: (i) the definition of a cycling strategy and (ii) the closure at each level.

Terracol *et al.* have proposed a V-cycle algorithm [21, 22, 23], based on a fixed or self-adaptive evaluation of the integration time on each grid, together with an extension of dynamic mixed model or a hierarchical closure. The tests show a reduction of the CPU time by a factor up to 5 (compared to monolevel LES on the same grid) without noticeable loss on the accuracy of the results for the plane channel flow and the plane mixing layer.

5.2. ZONAL RANS/LES COUPLING

A first way to couple RANS and LES is to define a zonal approach, as it is implicitely done in the Detached Eddy Simulation approach. From a theoretical point of view, this way of coupling RANS and LES appears as an extension of the zonal multiresolution LES algorithm discussed above in the paper. This analysis is conducted by Quéméré *et al.* [21, 19]. The main new points are: (i) RANS and LES solutions do not correspond to the same effective filter (that can be analyzed in the same way as LES effective filters [14]); (ii) RANS and LES solutions do not necessarily have the same dimension and (iii) the number of unknown is not the same if turbulence models based on transport equations are used.

An interface treatment for zero-equation SGS model and two-equations turbulence model has been assessed on the plane channel configuration, with reliable results on the mean velocity and the resolved Reynolds stresses. Examples of computed resolved Reynolds stresses for the plane channel con-

figurations are shown in Fig. 7. Two configurations have been investigated: near-wall RANS subdomain with LES domain at the center of the channel, and near-wall LES computation with RANS domain at the center of the channel.

5.3. ANOTHER RANS/LES COUPLING: THE NLDE APPROACH

The last point discussed in this paper deals with the reconstruction of turbulent fluctuations around a mean profile obtained using the RANS approach. An approach has recently been developped by Labourasse *et al.* [21, 10], which belongs to the Non-Linear Disturbance Equations family, as defined by Morris and his co-workers [16].

The idea is here to reconstruct locally the turbulent fluctuations for particular purposes (aeroacoustics, aero-optics) using a LES-like equations for the fluctuations, with source terms corresponding to the coupling with the mean flow. Assessment in the fully general compressible case, including unsteady mean flow, on the channel flow configuration is given in Ref. [10]. These results also show that the NLDE approach is more robust than classical LES. Examples of reconstructed resolved Reynolds stresses are compared to classical LES solutions in Fig. 8.

Acknowledgements

The author would like to emphasize the contribution of all his co-workers during the five past years: I. Mary, E. Garnier, P. Quéméré, M. Terracol, E. Lernormand, B. Raverdy, E. Labourasse, Ph. Guillen.

References

1. Sagaut, P., (2001) *Large-eddy simulation for incompressible flows.* Springer-Verlag, Berlin.
2. Boris, J.P., Grinstein, F.F., Oran, E.S., Kolbe, R.L., (1992) New insights into large-eddy simulation. *Fluid Dyn. Res.* 10, pp.199–228
3. CITS annual technical report (chapter 2.4), (2000), Stanford University
4. Ducros, F., Ferrand, V., Nicoud, F., Weber, C., Darracq, D., Gacherieu, C., Poinsot, T., (1999) Large-eddy simulation of shock/turbulence interaction. *J. Comput. Phys.* 152, pp. 517–549
5. Fureby, C., Grinstein, F.F., (1999) Monotonically integrated large-eddy simulation of free shear flows. *AIAA Journal* 37(5), pp.544–556
6. Garnier, E., Mossi, M., Sagaut, P., Deville, M., Comte, P. (1999) On the use of shock-capturing schemes for large-eddy simulation. *J. Comput. Phys.* 153, pp. 273–311
7. Garnier, E., Sagaut, P., Deville, M., (1999) Large-eddy simulation of shock/turbulence interaction. *Computers & Fluids, to appear*
8. Garnier, E., Sagaut, P., Deville, M., (2001) A class of explicit ENO filters with application to unsteady flows. *J. Comput. Phys.* 170, pp. 184–204

9. Garnier, E., Sagaut, P., Deville, M., (2000) Large-eddy simulation of the shock/boundary layer interaction. *submitted to AIAA Journal*
10. Labourasse, E., Sagaut, P., (2001) Reconstruction of turbulent fluctuations using a hybrid RANS/LES approach. *submitted to J. Comput. Phys.*
11. Lenormand, E., Sagaut, P., Ta Phuoc, L. (2000) Large eddy simulation of subsonic and supersonic channel at moderate Reynolds number. *Int. J. Numer. Methods Fluids* 32, pp. 369–406
12. Lenormand, E., Sagaut, P., Ta Phuoc, L., Comte, P. (2000) Subgrid-scale models for large-eddy simulation of compressible wall bounded flows. *AIAA Journal* 38(8), pp. 1340–1350
13. Liu, C., Liu, Z., (1995) Multigrid mapping in box relaxation for simulation of the whole proces of flow transition in 3D boundary layers. *J. Comput. Phys* 119, pp. 325–341
14. Magnient, J.C., Sagaut, P., Deville, M., (2001) A study of build-in filter for some eddy-viscosity models in Large-Eddy Simulation, *Phys. Fluids* 13(5), pp. 1440–1449
15. Mary, I., Sagaut, P., (2001) Large-eddy simulation of flow around an airfoil near stall. *submitted to AIAA Journal*; also AIAA Paper 2001-2559
16. Morris, P.J., Long, L.N., Bangalore, A., Wang, Q., (1997) A parallel three-dimensional computational aeroacoustics method using nonlinear disturbance equations. *J. Comput. Phys.* 133, pp. 56
17. Mossi, M., Sagaut, P., (2001) Numerical investigation of fully developped channel flow using shock-capturing scheme. *Computers and Fluids, to appear*
18. Quéméré, P., Sagaut, P., Couaillier, V., (2001) A new multidomain/multiresolution method for large-eddy simulation. *Int. J. Numer. Methods Fluids* 36, pp. 391–416
19. Quéméré, P., Sagaut, P., (2001) Zonal multi-domain RANS/LES simulations of turbulent flows. *submitted to Int. J. Numer. Methods Fluids*
20. Sagaut, P., Montreuil, E., Labbé, O., (1999) Assessment of some self-adaptive SGS models for wall bounded flows. *AST* 3(6), pp. 335-344
21. Sagaut, P., Labourasse, E., Quéméré, P., Terracol, M. (2000) Multiscale approaches for unsteady simulation of turbulent flows. *Int. J. Nonlinear Sciences and Numerical Simulation* 1(4), pp. 285–298
22. Terracol, M., Sagaut, P., Basdevant, C., (2001) A multilevel algorithm for large-eddy simulation of turbulent compressible flows. *J. Comput. Phys.* 167, pp. 439–474
23. Terracol, M., Sagaut, P., Basdevant, C., (2000) A time self-adaptive multilevel algorithm for large-eddy simulation with application to the compressible mixing layer. *submitted to Phys. Fluids*

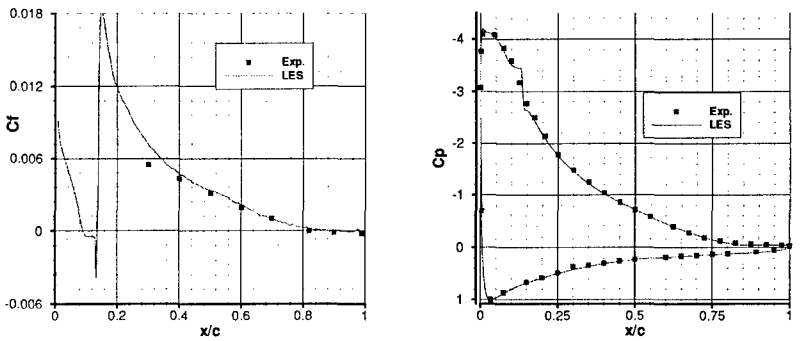

Figure 1. Flow around a 2D airfoil near stall - Skin friction (Left) and Pressure (Right) coefficients. Line: LES, Symbols: experiments

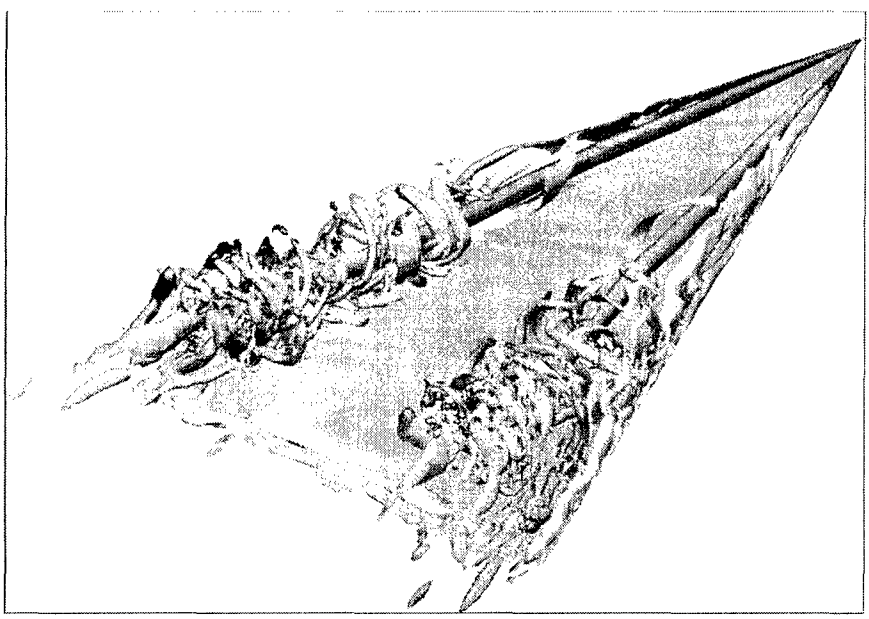

Figure 2. Flow around a Delta wing with vortex breakdown (instantaneous vorticity and pressure iso-surfaces)

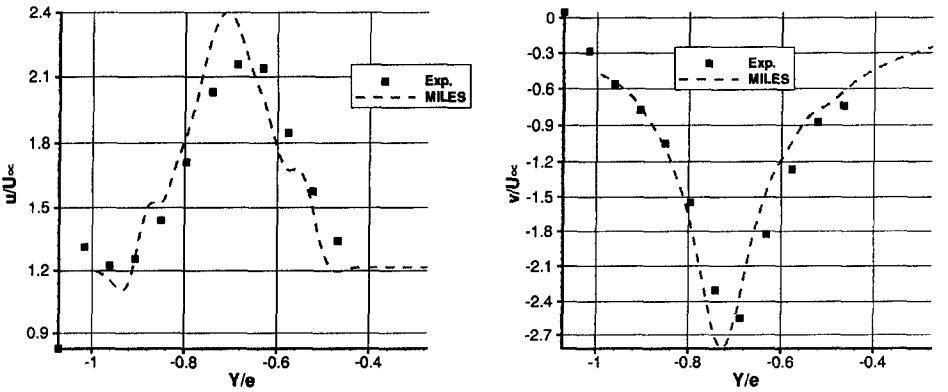

Figure 3. Flow around a Delta wing with vortex breakdown - Mean streamwise velocity (Left) and mean spanwise velocity (Right) profiles downstream the breakdown. Line: LES, Symbol: experiments

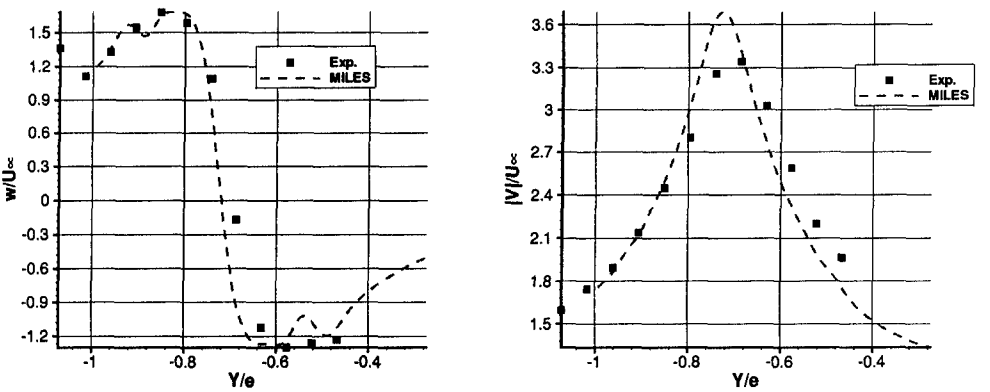

Figure 4. Flow around a Delta wing with vortex breakdown - Mean wall-normal velocity (Left) and mean velocity modulus (Right) profiles downstream the breakdown. Line: LES, Symbol: experiments

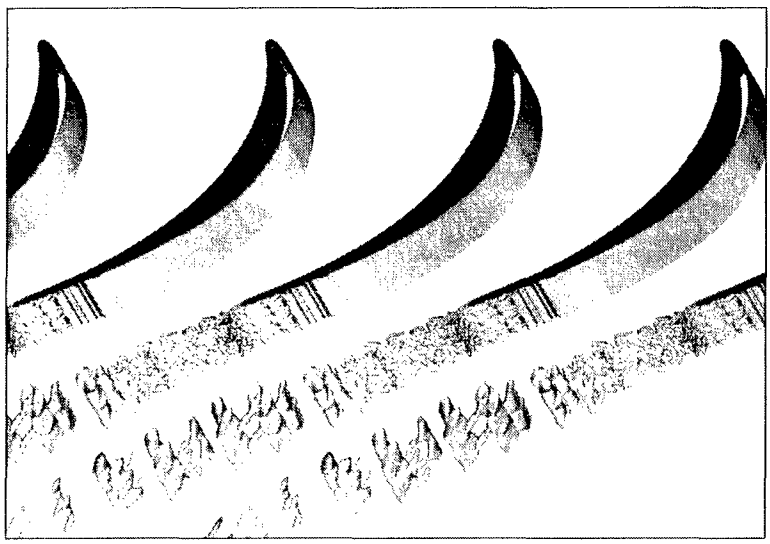

Figure 5. Flow around a low-pressure turbine blade (instantaneous vorticity iso-values)

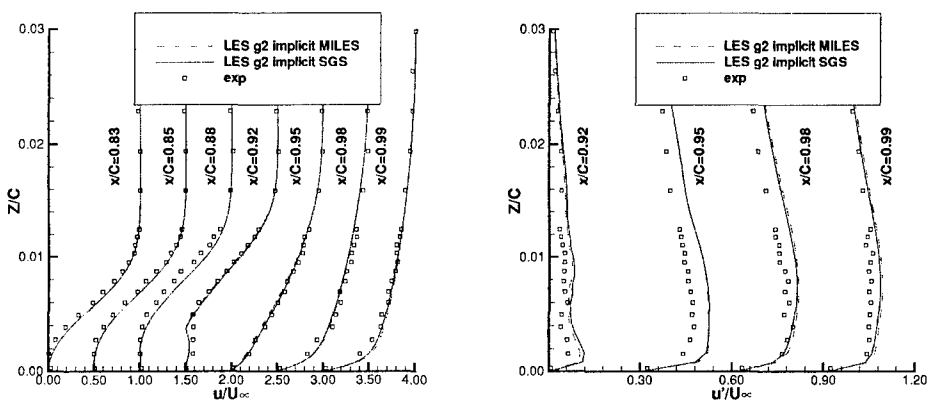

Figure 6. Flow around a low-pressure turbine blade. Mean velocity profile (Left) and RMS velocity profile (Right). Line: LES, Symbols: experiments

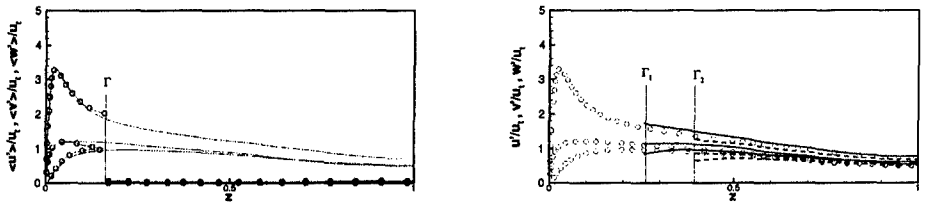

Figure 7. Zonal RANS/LES coupling - Channel flow, $Re_\tau = 590$ - Streamwise, spanwise and wall-normal *rms* velocity fluctuations. Near-wall LES treatment with RANS subdomain at the center of the channel; line: classical LES, symbols: coupled simulation (Left) and near-wall RANS simulation with LES domain at the center of the channel; symbols: classical LES, lines: coupled simulation (Right). Vertical lines note the position of the interface.

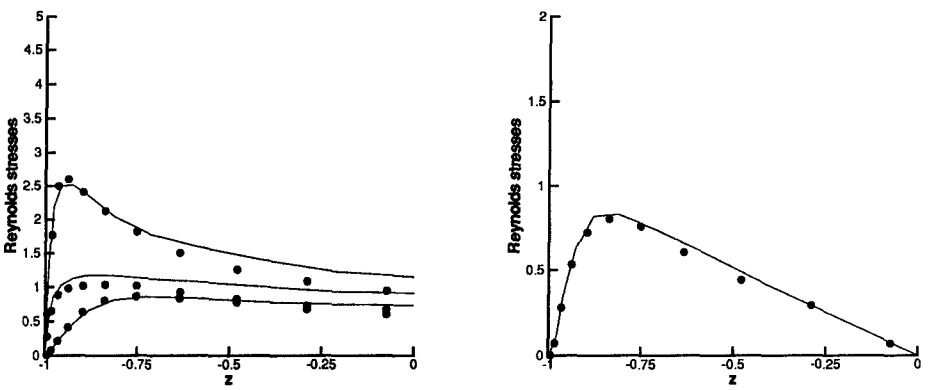

Figure 8. RANS/LES coupling - NLDE Approach - Channel flow, $Re_\tau = 395$ - Streamwise, spanwise and wall-normal *rms* velocity fluctuations (Left) and shear stress (Right). Line: NLDE, Symbol: classical LES